Journal of The Electrochemical Society, **147** (10) 3775-3784 (2000)
S0013-4651(99)11-096-6 CCC: $7.00 © The Electrochemical Society, Inc.

Effect of Substrate on Polyaniline Film Properties
A Cyclic Voltammetry and Impedance Study

Huyen N. Dinh[a,*] and Viola I. Birss[,z]**

Department of Chemistry, University of Calgary, Calgary, Alberta Canada T2N 1N4

The electrochemical properties of polyaniline (PANI) films, grown using multicycling methods, but using two different upper limits, have been examined in detail at three different substrates [Au, Pt, and glassy carbon (GC)]. Overall, type I films are only weakly dependent on the substrate employed. Even so, impedance measurements have shown that type I PANI films (grown by cycling between 0 and *ca.* 1 V in 0.1 M aniline + 1 M H_2SO_4), formed on Pt and Au, exhibit the most rapid growth rate, while the highest film pseudocapacitance per unit charge is seen for Pt substrates. Type I PANI has a porosity of 45-50% when formed on Pt and Au, but the porosity is much higher (*ca*. 77%) on GC, inversely correlated with film growth rate. The substrate has a more pronounced effect on the electrochemical properties of type II PANI films (grown by cycling between 0 and 1.7 V in 0.02 M aniline + 1 M H_2SO_4 solution). This is because type I films are formed at potentials at which PANI is conducting, while type II are formed primarily when PANI is insulating. Therefore, type I film growth occurs predominantly at the conducting PANI/solution interface, while growth of type II films occurs primarily at the underlying metal/solution interface, causing the substrate properties to become more significant. The growth rate of type II PANI is most rapid on GC, due to the absence of a barrier oxide film, *vs.* on Pt and Au.

Manuscript submitted November 29, 1999; revised manuscript received May 4, 2000.

Polyaniline (PANI) films have been studied independently on many different substrates, including Pt,[1,2] Au,[3,4] Pd,[5] C,[6,7] Al,[8] Zn,[9] Cu,[10] stainless steel,[11] TiO_2,[12] SnO_2,[13] and RuO_2.[14] However, only a few publications exist which, in a consistent study, have studied the effect of the nature of the electrode surface on the PANI film properties using two or more substrate materials. For example, Boschi *et al*.[6] have compared, based on the PANI yield, the growth rates of PANI films formed by cycling to 1.05 V *vs*. SHE (type I) on Pt, stainless steel (SS), pyrolytic graphite (PG), glassy carbon (GC), and Au electrodes. They concluded that the sequence of the PANI film growth rate on these electrodes is Au > SS > Pt ≈ GC > PG.[6] These authors postulated that the low yield of PANI on PG may be related to blockage by competitively adsorbed ions.

Lin *et al*.[14] found that the polymerization rate of aniline on a Pt electrode was higher than on RuO_2, when PANI was formed by cycling the potential between 0 and 1 V *vs*. SHE (type I). They suggested that the strong adsorption of aniline on the RuO_2 surface retarded the polymerization rate. When PANI growth was carried out by cycling the potential between 0 and 1.42 V *vs.* SHE, however, the relative rates of formation were reversed and the resulting PANI film on both surfaces was less stable and contained a significant fraction of degradation products (*e.g.*, benzoquinone, BQ).[14] These studies have indicated that the choice of substrate is a key factor in determining the growth rate, structure, and electrochemical behavior of PANI films. Therefore, in the present work, a more careful study of PANI film growth on three different substrates, Au, Pt, and GC, was carried out and the properties of the resulting films have been compared. The impact of the substrate is shown to be most significant when new growth of PANI occurs at the underlying metal surface, as is the case for type II PANI (formed using higher potentials of *ca*. 1.7 V, where PANI is insulating). The substrate effect on the PANI film properties is much less significant for type I PANI (film growth occurs on the outer PANI surface, as it is in its conducting state at *ca*. 1 V).

Experimental

Instrumentation.—The details of the solutions and the instrumentation used for carrying out cyclic voltammetry (CV) have been described elsewhere.[15] The impedance data, collected for PANI films formed on Pt and GC electrodes, were acquired using Solartron 1255/1287 instruments, run by Z-plot 2.0 software (Scribner Associates) and were analyzed using a Zview (version 2.0, Scribner Associates) fitting program. However, the data for PANI films formed on Au were collected using the Solartron 1255/1286 combination, driven by Z-Plot 1.6 software (Scribner Associates), and analyzed with EQUIVCRT software, written by Boukamp.

All impedance data were collected in a fresh, deoxygenated 1 M H_2SO_4 solution, at fixed dc potentials ranging from 0.1 to 0.6 V *vs*. RHE for PANI films on Au and Pt electrodes, and from −0.3 to 0.6 V *vs*. RHE for PANI films on GC. Normally, a sinusoidal 10 mV rms potential amplitude and frequencies from 65 or 100 kHz, to 1 or 0.1 Hz, logging down 12 points per decade, were employed.

Cells and electrodes.—Standard three-electrode, two-compartment cells were used for PANI growth and ac impedance measurements. The working electrode (WE) was either a polycrystalline Au or Pt wire (Aldrich, 99.99%, 0.5 mm diam), or a GC disk (apparent area of 0.95 cm^2). The counter electrode was a large area Pt gauze and the reference electrode (RE) was a reversible hydrogen electrode (RHE). For impedance measurements, a fourth, pseudo-reference electrode (also a Pt gauze) was placed in the WE compartment and was electrically connected to the RE via a 6.8 μF capacitor to reduce artifactual phase shifts at high frequencies.[16]

All potentials in this paper are reported *vs.* the RHE and the current and charge densities are given with respect to the real electrode area, except for the GC case, where the apparent electrode area was used. The method for determining the real electrode area of Au and Pt electrodes has been described elsewhere.[17]

After each experiment, the PANI film was removed from the Au and Pt wire electrodes by sonicating the PANI-coated WE in a 30% hydrogen peroxide solution for several hours. The electrode was then rinsed with triply distilled water and stored in 10% v/v H_2SO_4 solution. Before the growth of a fresh PANI film, the Au and Pt wires were further cleaned by potential cycling between −0.05 and 1.90 V at 1 V s^{-1} in 1 M H_2SO_4 for about 20 min. For the GC electrode, the PANI film was removed by first polishing with wet 600 grit emery paper and then with alumina/water suspensions (1, 0.3, and 0.05 μm, E.T. Enterprises), using a polishing cloth, until a mirror-like surface was obtained. The polished GC electrode was then immersed in a triply distilled water bath and sonicated for several minutes to remove any polishing residue.

Polyaniline growth.—PANI films were grown to various thicknesses on the polycrystalline Au wire or GC disk electrodes by cycling the potential at 100 mV s^{-1} (or 50 mV s^{-1}) for controlled periods of time between 0 and 1 V in 0.1 M aniline + 1 M H_2SO_4

* Electrochemical Society Student Member.
** Electrochemical Society Active Member.
[a] Present address: Los Alamos National Laboratory, Los Alamos, NM 87545, USA.
[z] E-mail: birss@ucalgary.ca

S0013-4651(99)11-096-6 CCC: $7.00

solution (type I film) or between 0 and 1.7 V in 0.02 M aniline + 1 M H_2SO_4 solution (type II film). On Pt, PANI films were grown by using 0.05 V as the lower limit for both type I and II films. The thickness of both types of PANI film on all substrates was obtained from the integration of slow sweep CVs between 0 and 0.8 V *vs*. RHE and using the relationship of 500 C per cm^3 of film, determined from our prior ellipsometry and quartz crystal microbalance (QCMB) results for type I PANI films on Au.[18] These film thicknesses should be viewed as approximate only, as types I and II films are shown in the present work to have slightly different porosities on the different substrates under study.

Results and Discussion

CV Response of Type I PANI Film Growth on Au, Pt, and GC Electrodes

Figure 1 shows the CV response of type I PANI films grown on the three substrates under study here. Commencing with Au, Fig. 1a shows the CV response in 0.1 M aniline + 1 M sulfuric acid solution after various times (between *ca*. 15 and 120 min) of PANI film growth in the aniline/sulfuric acid solution. The CVs of these films display A_1 and C_1 peak potentials at 0.42 and 0.3 V, respectively, which remain essentially constant with increasing film thickness. These peaks are associated with the oxidation/reduction of the leucoemeraldine/emeraldine states of PANI. Figure 1a also shows no evidence for the presence of any PANI decomposition products [*e.g.*, benzoquinone (BQ)] in the film, detected as a pair of redox peaks centered at *ca*. 0.75 V.[19]

Figure 1b shows that the CV response and growth rate of type I PANI films (after *ca.* 85 to 125 min of growth) on a Pt substrate are very similar to that on Au. Type I PANI growth on either Pt or Au required about 2 h to produce a film thickness of 160 nm. It is clear that the choice between Au and Pt substrates does not affect the rate or CV characteristics of type I PANI film growth.

One of the reasons for selecting GC in this study was that it is nonmetallic, so that differences in the interactions between metallic *vs.* nonmetallic substrates and PANI could be investigated. GC is considered to consist of planar aromatic structures and, depending on the nature and duration of the treatment, different carbon/oxygen ratios and oxygen-containing functional groups, such as carboxyl, carbonyl, and hydroxyl, can be found on its surface.[20] For example, when GC is activated by cycling to anodic potentials greater than *ca*. 2.7 V, [21] or is cycled between 2.7 and −0.8 V, a porous, hydrated, and nonconductive oxide film, containing quinone-like groups and carboxylic acid functionalities, is generated.[21,22]

The CV response for type I PANI films electrodeposited on a GC electrode for various times is shown in Fig. 1c. It was found that the time required to achieve a particular quantity of PANI on GC depends on the electrode surface pretreatment, and therefore can vary between experiments. Also, type I PANI film growth is notably slower at GC than at Pt or Au. This is demonstrated by the fact that more than three cycles to 1.05 V, the condition normally used to initiate PANI growth on Au or Pt, and sometimes several scans to potentials even up to 1.1 V, are required to initiate type I PANI growth on GC substrates. Further film thickening of type I PANI film growth continues to be slower at GC that at Pt or Au substrates. The presence of aromatics, carbonyl, and carboxyl groups on the nonmetallic GC surface are likely the reason that type I PANI growth on GC is comparatively slow. Aniline may be more strongly adsorbed on the surface groups present on the GC surface, similar to the case of RuO_2. [14] This stabilization of aniline in the adsorbed state may, in turn, diminish the rate of monomeric aniline oxidation to the corresponding radical cation, resulting in slower PANI growth on GC. It is also possible that PANI nuclei form only at defect sites on the oxide-coated GC substrate, and thus few sites are present for subsequent PANI growth.

Similar to Au and Pt (Fig. 1a and b), the peak potentials (A_1/C_1) and peak separation remain constant and there is no evidence for the formation of any PANI decomposition products during type I film growth on GC (Fig. 1c). Contrary to the case at these two metals, the BQ peaks are not seen in the first few CV cycles during growth at GC, although higher anodic potentials were used to initiate PANI growth. Further, the prepeak (A_0) is seen to be located at a slightly more cathodic potential, *ca*. 0.2 V, at GC, than observed for type I PANI on Au (0.25 V) or Pt (0.23 V).

Overall, the small differences in the potential of the anodic prepeak for the three different substrates and the differences in the first few type I PANI film growth cycles (the absence of BQ peaks and the slower polymerization rate of PANI on GC) are the only apparent effects of the change in electrode substrate. Cycling the potential to no more than 1.0 V ensures that PANI growth, which begins at *ca*. 0.8 V, will occur only when PANI is in its fully conducting state. Under these conditions, the applied potential will fall across the PANI/solution interface and growth of new PANI should occur on the outer film surface. This would explain why, other than in the first few cycles of potential when not all of the substrate would yet be covered

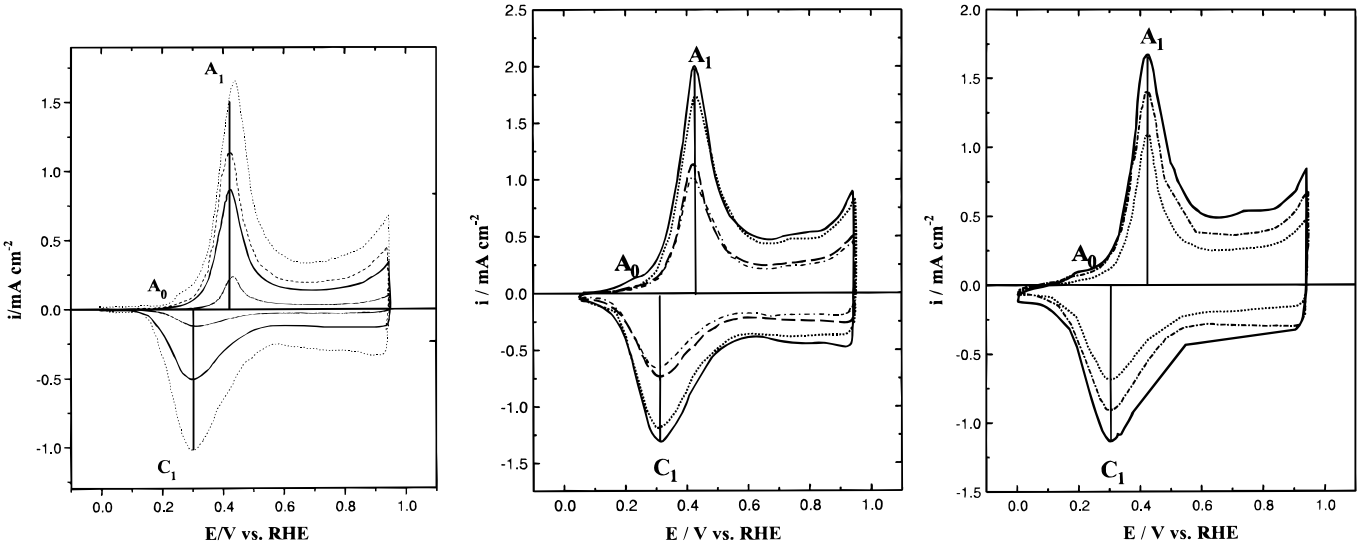

Figure 1. CV response for type I PANI film grown on Au (a), Pt (b), and GC (c) in 0.1 M aniline + 1 M H_2SO_4 by cycling at 50 mV s^{-1}. Film thicknesses (calculated using the ratio of 500 C cm^{-3}, and listed in order of increasing CV currents) are (a, left) 15, 60, 90, and 145 nm; (b, center) 70, 90, 145, and 160 nm; and (c, right) 80, 110, and 145 nm.

S0013-4651(99)11-096-6 CCC: $7.00

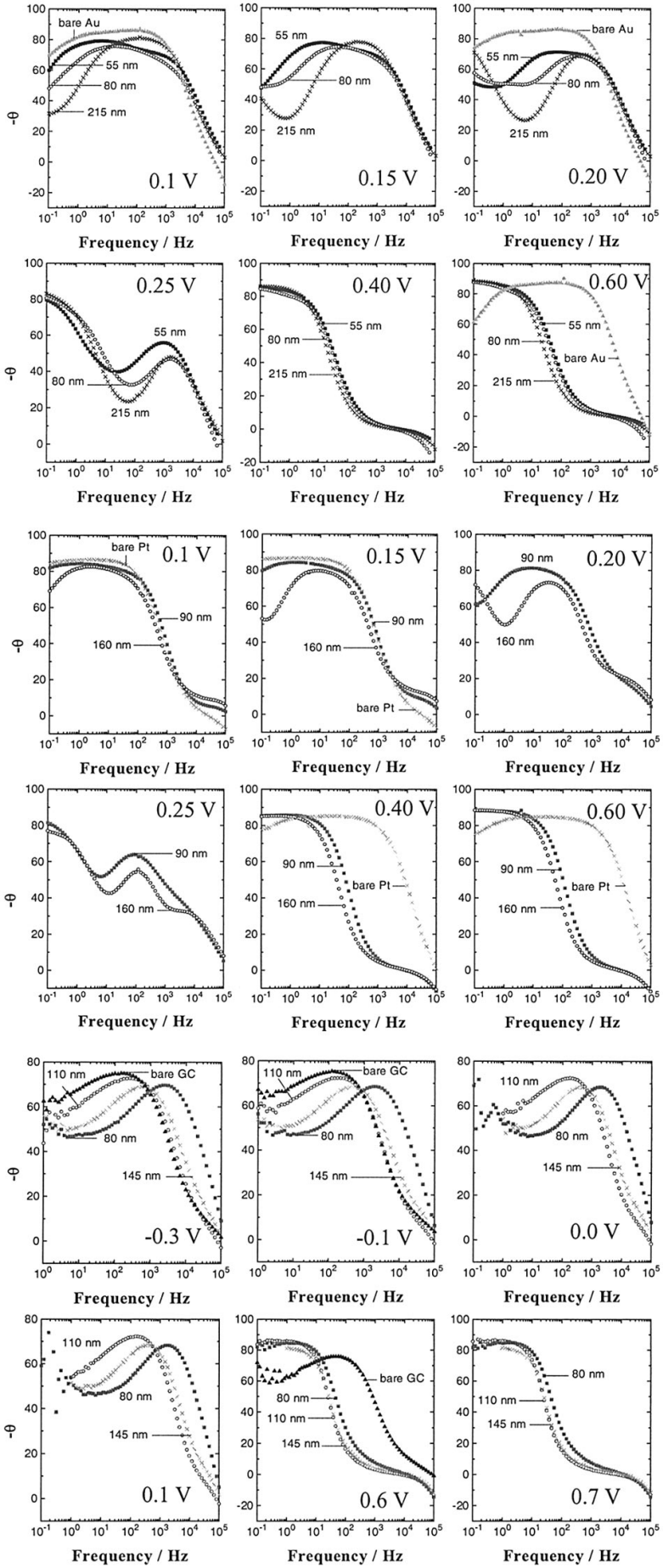

Figure 2. (a, top two rows) Series of phase angle Bode plots, collected during a scan in the anodic direction, for bare Au (▲) and type I PANI films on Au in 1 M H_2SO_4 as a function of potential and film thickness: 55 (■), 80 (○), and 215 nm (×).
(b, center two rows) Series of phase angle Bode plots, collected during a scan in the anodic direction, for bare Pt (×) and type I PANI films on Pt in 1 M H_2SO_4 as a function of potential and film thickness: 90 (■) and 160 nm (○).
(c, bottom two rows) Series of phase-angle Bode plots, collected during a scan in the anodic direction, for bare GC (▲) and type I PANI films on GC in 1 M H_2SO_4 as a function of potential and film thickness: 80 (■), 110 (○), and 145 nm (×).

S0013-4651(99)11-096-6 CCC: $7.00

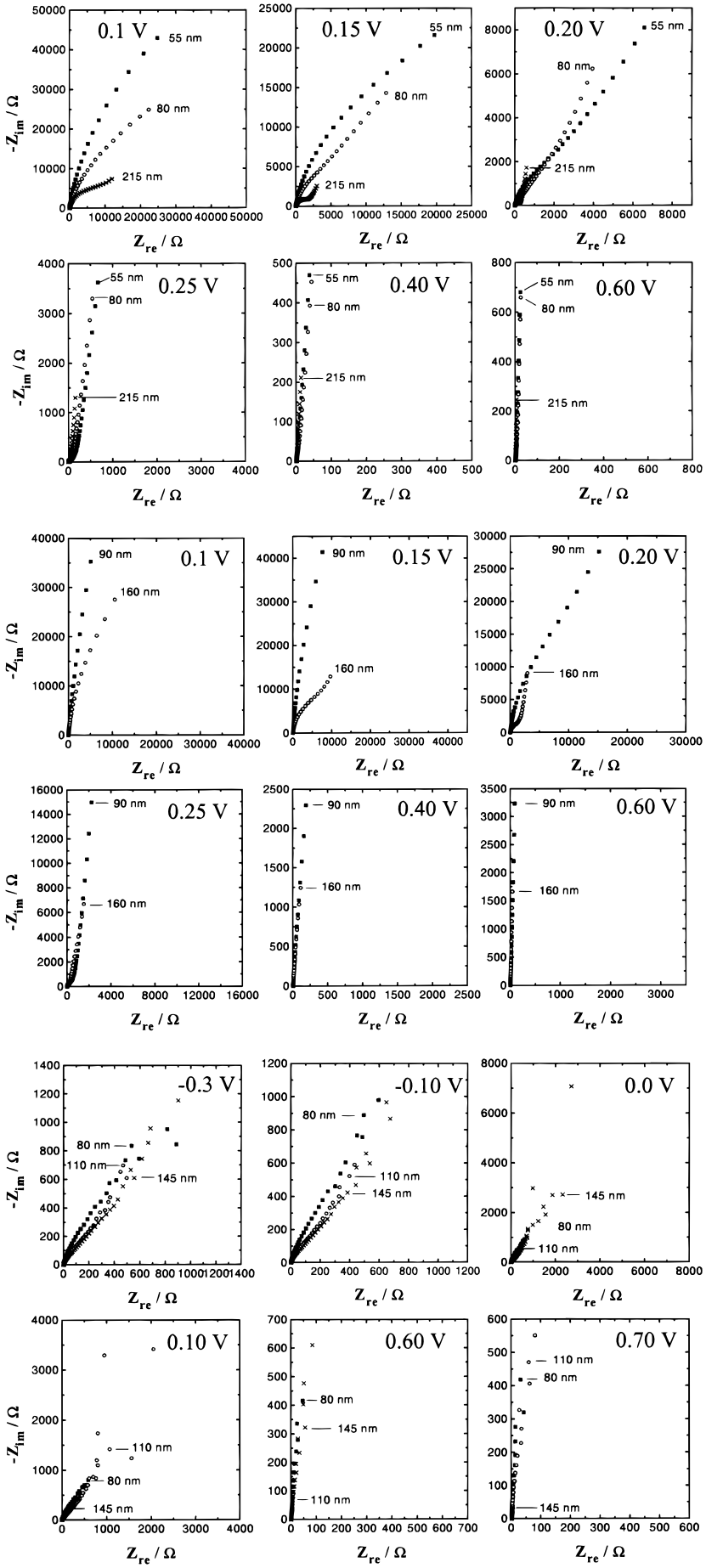

Figure 3. (a, top two rows) Series of Nyquist plots, collected during a scan in the anodic direction, for type I PANI films on Au in 1 M H_2SO_4 as a function of potential and film thickness: 55 (■), 80 (○), and 215 nm (×).
(b, center two rows) Series of Nyquist plots, collected during a scan in the anodic direction, for type I PANI films on Pt in 1 M H_2SO_4 as a function of potential and film thickness: 90 (■) and 160 nm (○).
(c, bottom two rows) Series of Nyquist plots, collected during a scan in the anodic direction, for type I PANI films on GC in 1 M H_2SO_4 as a function of potential and film thickness: 80 (■), 110 (○), and 145 nm (×).

S0013-4651(99)11-096-6 CCC: $7.00

by PANI film, there appears to be only a negligible effect of the substrate on the CV response during the growth of type I PANI films.

Comparative EIS Studies of Type I PANI Films on Au, Pt, and GC Electrodes

General impedance response at all substrates.—Following PANI film growth, the electrodes were transferred to aniline-free 1 M sulfuric acid solutions, and impedance data for type I films on Au, Pt, and GC electrodes were collected at various potentials. The Bode depictions (phase angle only) of the raw impedance data, obtained as a function of potential for the bare substrate and for type I PANI films on Au, Pt, and GC, are shown in Fig. 2a–c, respectively, while the Nyquist representation of this data is shown in Fig. 3a–c. It has been demonstrated in parallel work that the impedance data for the reduced and intermediate forms of PANI films are different, at any potential, depending on the direction that the potential is changed, positively or negatively.[23] The data in Fig. 2 and 3 were all collected starting at 0.1 V (or −0.3 V for GC) and ending at 0.6 V (or 0.7 V).

At low potentials, PANI is in its reduced, insulating state, and it would therefore be expected that the electrochemical response will originate from the underlying metal/solution interface at the base of the PANI film pores.[17,23] However, Fig. 2 shows that, at 0.1 V, the impedance response of the insulating form of PANI film does change notably with film thickness on both Au (Fig. 2a) and GC (Fig. 2c). On Au, the change in the impedance response at low frequencies, in particular, appears to track the PANI film thickness, perhaps reflecting a trend in the film porosity with increasing thickness. In the case of GC, however, the direction of change of the impedance response of PANI is random with film thickness, and is the same at −0.1 and −0.3 V. This may reflect either a more chaotic PANI film pore structure, or that the properties of the GC substrate between experiments are variable, as indicated earlier. In the case of Pt (Fig. 2b), the impedance response of the reduced form of PANI is close to that of the underlying substrate, until relatively thick films are formed, similar to the situation at Au.

At intermediate potentials from 0.15 to 0.30 V, the Bode phase angle plots for type I PANI on all three substrates show that a second time constant, appearing at low frequencies, becomes more defined as the PANI film is converted from the insulating, reduced to the intermediate, partially conducting state. This indicates the onset of the PANI redox reaction.

At high potentials, *e.g.*, 0.4-0.6 V, the Bode plots for PANI on Au, Pt, and GC all show the highly capacitive nature of the oxidized, conducting PANI film (Fig. 2a, b, and c). When PANI is in this state, the film pseudocapacitance dominates the impedance response.[17,23] In the Nyquist format (Fig. 3a, b, and c), this is seen as a near-vertical line at low frequencies.[17] The phase angle at 0.1 Hz (Fig. 3), for example, indicates that conducting type I PANI films on Pt (88°) and Au (88°) respond in a more purely capacitive fashion than on GC (80 to 85°). However, this could also arise from a greater degree of roughness of the GC substrate and hence of the PANI film. It should be pointed out that an inductive effect (positive phase angles) is seen at high potentials for conducting PANI at all substrates. This has been shown to originate from the instrumentation,[23] and can therefore be ignored.

Overall, similar to the impact on the CVs, the substrate effect on the impedance response appears to be minor for type I PANI films, based on the raw data. At low potentials (0.1 V), the impedance response for type I PANI films on Pt and Au shows a similar trend with film thickness. However, PANI films deposited on Pt and Au are somewhat more capacitive than on GC.

Equivalent circuit approach and interpretation.—The impedance data for the nonconducting, fully reduced form (0.10-0.15 V) of type I PANI films on Au, Pt, and GC were fitted to the equivalent circuits (EC) shown in Fig. 5a, 6a, and 7a, respectively, while the data for the oxidized form of the film (0.35-0.60 V) were fitted to the ECs shown in Fig. 5b, 6b, and 7b, respectively. This allows a more quantitative assessment of film properties. To obtain the best-fit, a constant phase element (*CPE*) was often used instead of a capacitor (*C*). A *CPE* is related to a capacitor through the relationship, $C = CPE^n$, where *n* can have a value between 0 and 1. When $n = 1$, the *CPE* is considered to be a pure capacitor. *n* values less than 1 are seen for the charging of a rough and/or porous electrode surface or in the presence of many inhomogeneities on an electrode surface.[24] A *CPE* with an associated *n* value of 0.5 is related to the well-known Warburg element, which represents diffusion controlled processes.

Figures 4-6 also show the overlay of the experimental and the fitted impedance data, based on the ECs shown, in the form of phase angle Bode plots for the reduced and oxidized PANI films. Data at frequencies greater than *ca.* 4 kHz were deleted for EQUIVCRT analysis, due to the presence of the inductive artifact,[23] mentioned above. Also, the impedance data for films which were neither fully conducting nor fully insulating, *i.e.*, over the narrow potential range of 0.20 to 0.30 V, could not be fitted well to any EC,[17,23] for all substrates, and therefore were not considered here.

Determination of type I PANI film coverage as a function of substrate.—The data obtained for type I PANI at the most negative potentials, when the film is fully reduced and electrically nonconducting, is considered first here. Starting with Au as the substrate, Fig. 4a shows a very good fit of the overlay to the EC shown for the 80 nm thick PANI film, yielding a small χ^2 value (χ^2 is the weighted sum or squares of the deviations of the nonlinear least square fit curves from the experimental points for a range of independent variables) of 2×10^{-3}. The R_1 element reflects the solution resistance between the surface of the PANI film and the RE [4,7,25,26] for all ECs shown in Fig. 4-6. CPE_1 in Fig. 4a reflects the charging of the Au/solution double layer at the base of the pores of the PANI film. CPE_2 arises from a small

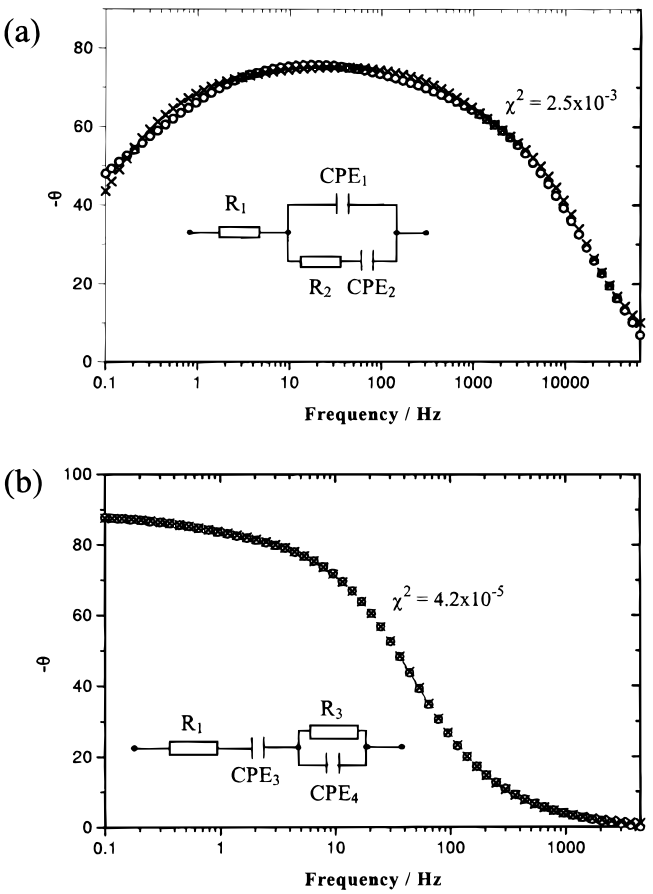

Figure 4. Typical phase-angle Bode plot for an 80 nm (a) reduced, insulating (0.1 Hz to 65 kHz) and (b) oxidized, conducting (0.1 Hz to 4.4 kHz) form of type I PANI film on Au at 0.1 and 0.6 V, respectively, collected in the anodic scan, in 1 M H_2SO_4. Both the experimental data (—○—) and the corresponding fit (—×—), based on the ECs shown in the figure, are given.

S0013-4651(99)11-096-6 CCC: $7.00

contribution from the PANI pseudocapacitive redox reaction, which must still be occurring to a minor extent at these negative potentials.[17] R_2 represents the resistance of the reduced, insulating PANI film and its pores.[17] As the assignment of these parameters has been discussed in detail elsewhere,[17] only the substrate/solution double-layer capacitance element (CPE_1) is discussed here and used to compare the properties of the reduced PANI films formed on the different substrates. Under these conditions, CPE_1 can provide insight into the coverage of the substrate by PANI, hence giving an indication of film porosity.[25-28]

Based on the overlays for all of the type I films studied at Au, at 0.1 V, CPE_1 has a value of *ca*. 20 μF cm^{-2} for the 55 nm film, 32 μF cm^{-2} for the 80 nm film, and 25 μF cm^{-2} for the thickest (215 nm) PANI film on Au, with associated n values in the range of 0.83 to 0.92.[17] By comparing these CPE_1 values with that of the double-layer capacitance of the bare Au/solution interface, found in this work to be 55-60 μF cm^{-2}, the fraction of the Au electrode which remains unblocked by the overlying type I PANI film, *i.e.*, the film porosity, is 45 ± 10% for these three films on Au.[17] No trend in the degree of blockage of Au with PANI film thickness is seen.

In the case of Pt as the substrate, the impedance data for type I PANI films in the reduced state were found to best-fit the EC shown in Fig. 5a. This EC is quite different from that used for type I PANI on Au (Fig. 5a). This may be due to the fact that the hydrogen underpotential deposition (upd) reaction can occur at Pt sites not blocked by PANI in the same potential range in which reduced PANI can be studied, as discussed above. CPE_1 is therefore considered to reflect the charging of the Pt/H upd/solution double layer at the base of the pores of the PANI film, while the additional CPE_2 element is again suggested to reflect a small contribution from the PANI pseudocapacitive redox reaction. R_2, associated with CPE_2, is again the resistance of the reduced, insulating PANI film, while R_3 may reflect the occurrence of some trace redox reactions, *e.g.*, oxygen reduction.

On Pt, CPE_1 at 0.1 V is 285 and 310 μF cm^{-2} for the 90 and 160 nm PANI films, respectively, with associated n values of 0.93. This relatively high capacitance arises from the pseudocapacitance associated with the adsorbed hydrogen redox chemistry. Prior to PANI film deposition, the capacitance of the polymer-free Pt/solution interface was determined, at the same potential, to be 590 μF cm^{-2}. By ratioing the CPE_1 values for all of the PANI coated *vs*. bare Pt electrodes, it is seen that 50 ± 2% of the Pt surface remains accessible to solution after type I PANI film formation. This suggests that these PANI films on Pt are of similar porosity to those formed on Au (45 ± 10%). Also, no trends in porosity can be discerned as a function of film thickness.

The overlay of the simulated and experimental impedance data for the reduced form of type I PANI films on GC is shown in Fig. 6a. An additional reason for the choice of GC as a substrate for impedance studies was that it has a high overpotential for the hydrogen evolution reaction (HER). Consequently, impedance data can be obtained at potentials more negative than 0.1 V without interference from the HER. It was anticipated that this would allow a more accurate estimation of PANI film coverage, as the PANI pseudocapacitive contribution should become zero at more negative potentials. This is in contrast to the case of Au and Pt, where it was seen (Fig. 4a and 5a, respectively) that the CPE_2 element was still present, even at 0.1 V.

Therefore, the coverage of type I PANI films on GC was established using this approach. The EC (Fig. 6a) used to fit the impedance data for the reduced form of PANI on GC is again different, but most similar to that used for type I PANI at Au (Fig. 4a), being similar in construction and having the same number of circuit elements.

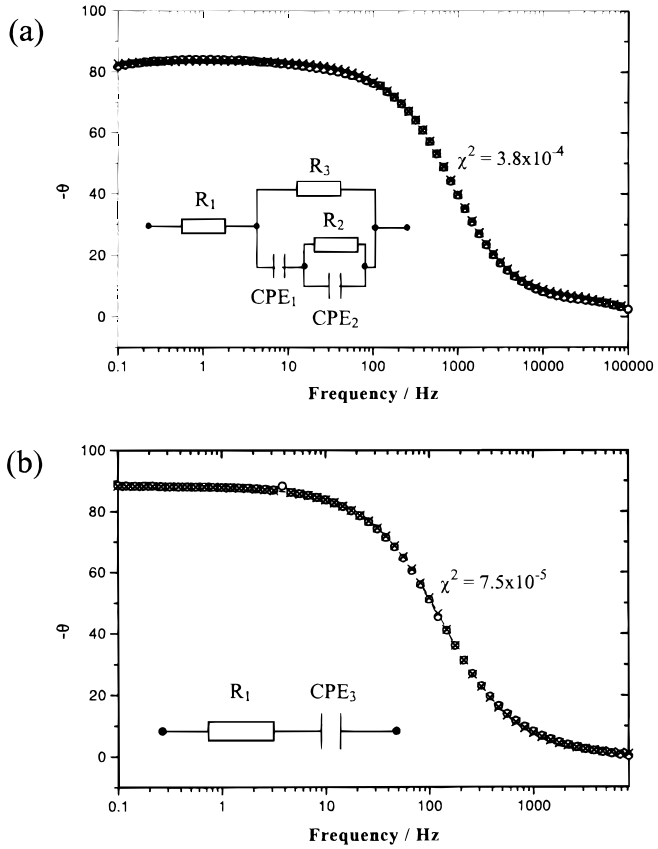

Figure 5. Typical phase-angle Bode plot for a 90 nm (a) reduced, insulating (0.1 Hz to 100 kHz) and (b) oxidized, conducting (0.1 Hz to 10 kHz) form of type I PANI film on Pt at 0.1 and 0.6 V, respectively, collected in the anodic scan, in 1 M H_2SO_4. Both the experimental data (—○—) and the corresponding fit (—×—), based on the ECs shown in the figure, are given.

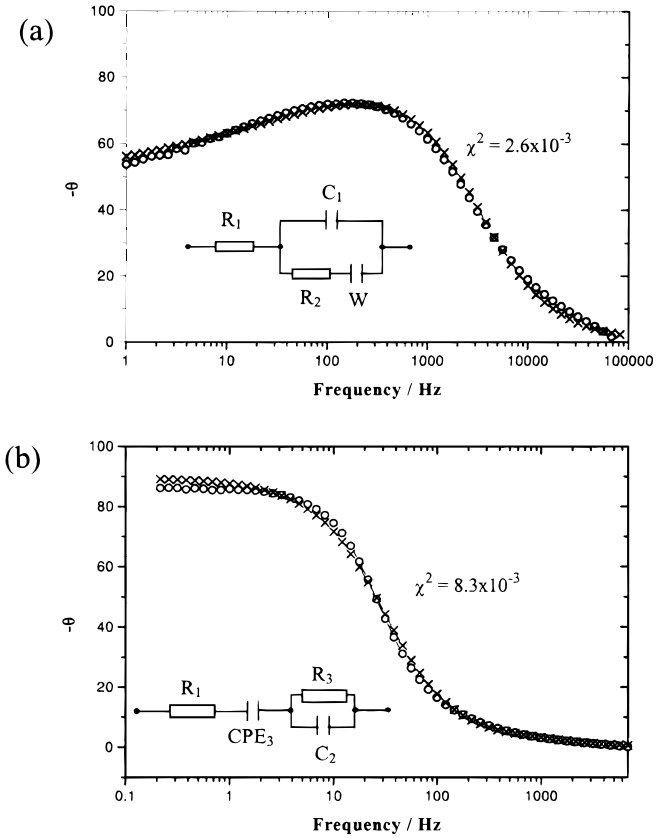

Figure 6. Typical phase angle Bode plot for a 110 nm (a) reduced, insulating (1 Hz to 68 kHz) and (b) oxidized, conducting (0.2 Hz to 6.8 kHz) forms of a type I PANI film on GC at 0.1 and 0.6 V, respectively, collected in the anodic scan, in 1 M H_2SO_4. Both the experimental data (—○—) and the corresponding fit (—×—), based on the ECs shown in the figure, are given.

S0013-4651(99)11-096-6 CCC: $7.00

R_2 is again the resistance of the reduced, insulating PANI film. However, the CPE_1 and CPE_2 elements, seen in Fig. 4a, have been replaced by a capacitance (C_1) and a Warburg element (W), respectively, in Fig. 6a. This difference likely arises from the unique surface properties and impedance response of the bare GC electrode, for which the best-fit EC in 1 M H_2SO_4 is a Randles circuit, containing a Warburg (W) element[29,30] (Fig. 6a) at all potentials. It is very interesting that, when a PANI film is present on the GC electrode and is examined in its fully reduced state (−0.3 to 0.1 V), the same Warburg-containing EC fits the data well (overlay in Fig. 6a). The Warburg element likely reflects transport limitations through the surface functionalities on the GC surface.

In order to determine the coverage of type I PANI at GC, similar to what was done at Pt and Au above, C_1 was examined at potentials down to −0.3 V. Figure 7 shows that the value of C_1 varies with potential and depends on the sweep direction. For example, for the 145 nm type I PANI film on GC, C_1 decreases from 18 to 13 μF cm^{-2} as the potential is changed cathodically and then increases from 12 to 14 μF cm^{-2} as the potential is changed anodically. As this sweep direction dependence of C_1 was also seen with bare GC, this appears to be a characteristic of the substrate pseudocapacitance, again confirming that the impedance response of reduced PANI films is largely that of the exposed substrate.

Therefore, the coverage of type I PANI films at GC was determined by ratioing the C_1 values for the bare and coated electrode at the same potential and in the same direction of potential change. This analysis shows that the average type I PANI coverage on GC is 22 ± 8%, increasing with film thickness, and that type I PANI films formed on GC are the most porous (77 ± 7%). Further, the trend of increasing type I PANI coverage (decreasing CPE_1) with film thickness was not seen at either Pt or Au. This supports the nucleation and growth mechanism for PANI on GC, in which the size of the deposits (nuclei) on the surface should increase in size with time of growth. This model of type I PANI film growth was suggested also by a parallel study of the kinetics of the HER at bare *vs*. PANI-coated electrodes.[17] It is also consistent with the difficulty of initiating type I PANI film growth at GC, which only certain surface sites are viable for this process.

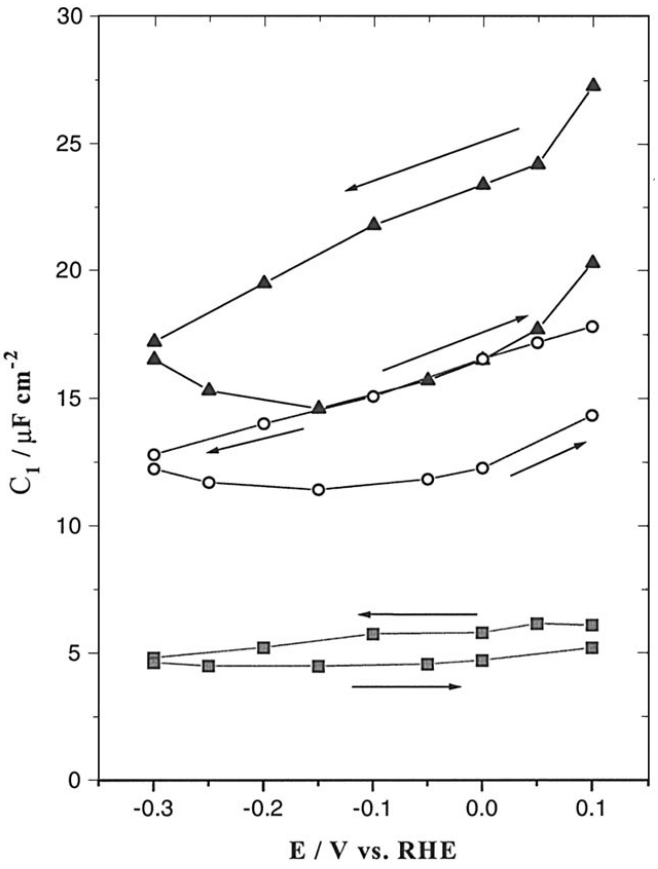

Figure 7. Double-layer capacitance (C_1) *vs*. potential plot for three reduced type I PANI films grown on GC disk in 1 M H_2SO_4: 80 nm (—■—), 110 nm (—●—), and 145 nm (—▲—). C_1 was obtained from fitting the impedance data (1 Hz-100 kHz), collected anodically and then cathodically, as indicated by the arrows, to the EC shown in Fig. 5a.

Comparison of pseudocapacitance of conducting type I PANI films as a function of substrate.—A comparison of the impedance-determined properties of the conducting form of type I PANI films, particularly the film pseudocapacitance, as a function of the electrode substrate can now also be made. Figure 4b shows a very good fit ($\chi^2 = 4 \times 10^{-5}$) of the experimental and simulated data for conducting type I PANI on Au. The EC consists of the solution resistance (R_1) in series with the PANI film pseudocapacitance (CPE_3), with n_3 values of 0.94-0.99, and an R_3-CPE_4 parallel pair. The value of CPE_3 is the same as the film pseudocapacitance, determined directly from the Nyquist data (capacitance extracted from the linear slope of the Z_{im} *vs*. 1/frequency (f) plot and the relation $C = -1/(2\pi f Z_{im})$ [17,23,31]), indicating that it accurately represents this parameter. The parallel R_3-CPE_4 pair in Fig. 4b appears at high frequencies (> 100 Hz or > 1 V s^{-1}) and has associated n values of close to 0.5. It therefore indicates transport limitations within the PANI film on Au, as insufficient time is available at high frequencies for all type I PANI sites to react.[17] When the high frequency data (>100 Hz) are omitted, the best-fit EC becomes simply the solution resistance (R_1) in series with the PANI film pseudocapacitance (CPE_3), identical to the EC reported by others for conducting PANI.[25,32,33]

In the case of Pt, the EC for the oxidized form of type I PANI consists simply of a series R_1-CPE_3 (Fig. 5b). The fact that the R_1-CPE_3 EC fits the data for conducting PANI films at Pt at all frequencies, *i.e.*, that there are no rate limitations at high frequencies, shows that the type I PANI film kinetics are more rapid, overall, at Pt than on Au (Fig. 4b). The slow sweep CV experiments did not reveal these differences, showing the additional information that can be obtained from ac impedance experiments.

The best-fit EC for oxidized type I PANI at GC consists of a series R_1-CPE_3 pair, in series with a parallel R_3-C_2 unit (Fig. 6b). This EC is most similar to that used for Au (Fig. 4b). The origin and meaning of the additional parallel R_3-C_2 unit for PANI at GC in Fig. 6b is not clear at this time. It does not reflect a high frequency transport limitation, as seen by the fact that it contains a capacitor ($n = 1$), rather than a CPE with $n \approx 0.5$, as was the case for PANI on Au. This R_3-C_2 unit (Fig. 6b) may, therefore, reflect some unique aspect of the GC substrate at these higher potentials. Notably, the removal of the parallel R_3-C_2 unit from the EC does not seriously affect the quality of the fit obtained between the experimental and calculated data ($\chi^2 = 1.1 \times 10^{-2}$ *vs*. 8.3×10^{-3}).

Overall, the type I PANI film pseudocapacitance (CPE_3) on GC, Pt, and Au is linearly related to film charge density, at constant potential, as shown in Fig. 8. For the same charge density, the pseudocapacitance for PANI films grown on GC (685 ± 6 mF/C) is very similar to that on Au (690 ± 14 mF/C), while the PANI film pseudocapactance (740 ± 15 mF/C) is the highest on Pt. This is consistent with Horányi *et al.*'s radiotracer and CV results, which showed that PANI films grown on Pt are electrochemically more efficient, *i.e.*, more of the PANI film sites formed on Pt are electroactive, than those formed on Au.[3]

It is interesting that, when the pseudocapacitance of conducting PANI films is determined by impedance techniques, it has been reported[4,25,29,32] that the measured value (C_{acZ}) is often substantially lower than that predicted from the cyclic voltammetric (CV) response, *i.e.*, from the current divided by the sweep rate ($C_{CV} = i/s$). This decrease in capacitance ($1\text{-}C_{acZ}/C_{CV}$) results from the small voltage amplitude perturbation used in ac impedance experiment.[31] Figure 9 shows the type I PANI film capacitance, obtained from both the CV analysis and from impedance for the three substrates under

S0013-4651(99)11-096-6 CCC: $7.00

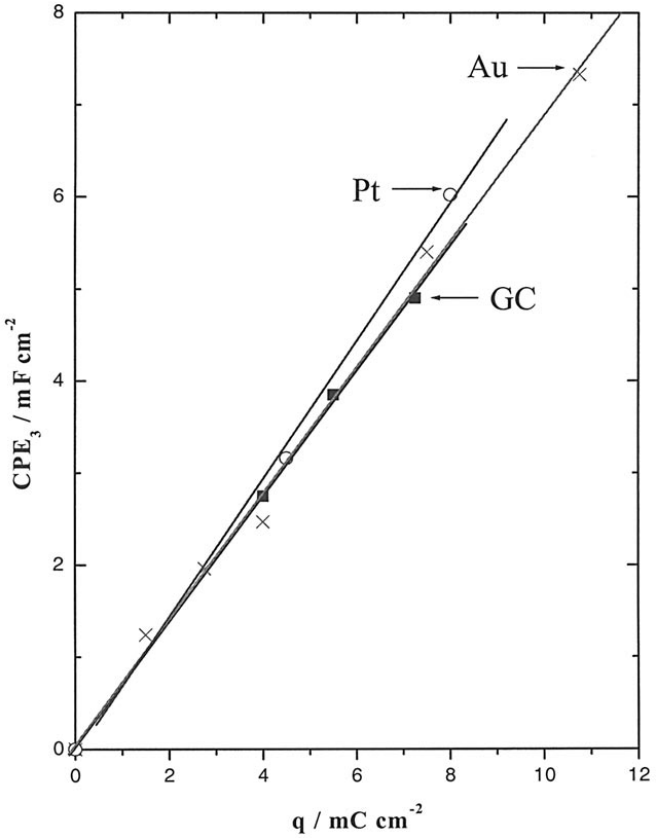

Figure 8. CPE_3 (at 0.6 V) for conducting PANI films on Au wire (×), Pt wire (○) and GC disk (■) electrodes and their line of best fit (—) as a function of charge density in 1 M H_2SO_4.

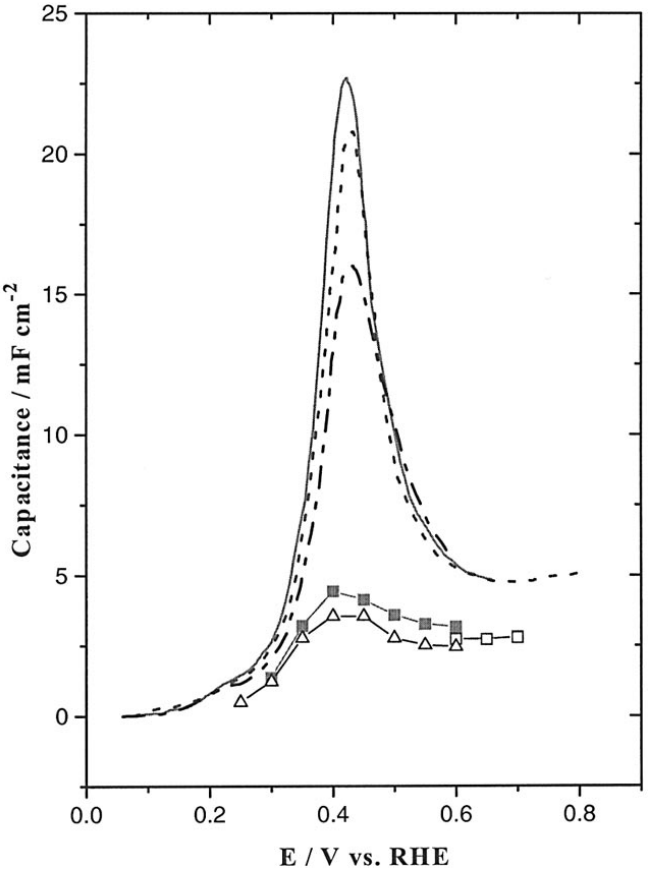

Figure 9. CV determined capacitance (*i*/*s*) and impedance-determined (1-12,000 Hz) CPE_3 value (see Fig. 5b, 6b, 7b) *vs*. potential for a 90, 80, and 80 nm type I PANI film grown on Pt wire (—), (—■—); Au wire (— – —), (—△—); and GC disk (- - -), (—□—), respectively, in 1 M H_2SO_4. *i*/*s* is represented by lines, while CPE_3 is represented by symbols joined by lines. For PANI on GC, only a few data points between 0.6 and 0.7 V were collected.

study. It can be seen that, at 0.6 V, for example, the type I PANI film pseudocapacitance, measured by impedance is 60, 40, and 50% of that determined by CV, on Pt, Au, and GC, respectively. This shows again that films grown on Pt substrates yield the highest capacitance when assessed using the ac impedance technique. It has been suggested[31] that this potential amplitude dependence of the capacitance is an indication that only certain polymer sites can change their conformation between the planar form of the oxidized PANI and the twisted form of the reduced film over a narrow potential range. Therefore, for small potential amplitudes, only a fraction of the polymer sites can react. Another explanation which has been suggested in our previous work is that, when the potential is cycled over a large potential range, water injection is delayed during PANI film oxidation, while water expulsion during reduction is more uniform with potential.[15] Therefore, based on the present study, PANI films grown on Pt may have a greater fraction of sites which are not susceptible to delays in water transport.[15]

Comparison of CV Response for Type II PANI Films on Au, Pt, and GC Electrodes

Unlike type I films, very different CV signatures are obtained during the growth of type II PANI films on Au, Pt, and GC electrodes (Fig. 10). It should be noted that a detailed CV and ac impedance comparison between type I and type II PANI films, all grown on the same substrate (Au), has already been published.[17] This work showed that type II films are formed at a much more rapid rate, con-

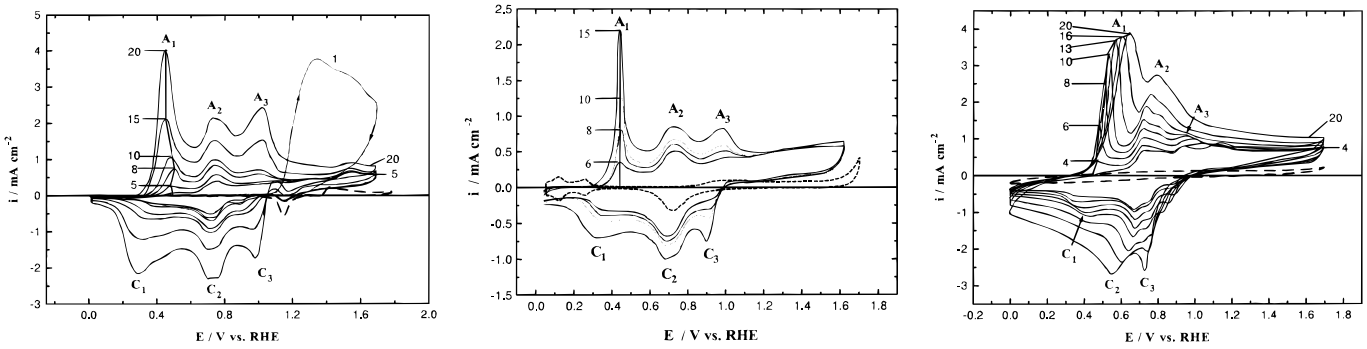

Figure 10. Typical set of CVs obtained during growth of type II PANI film on Au (a), Pt (b) and GC (c) in 0.02 M aniline + 1 M H_2SO_4, cycled at 100 mV s^{-1}. Also shown is the CV response of the bare substrate in 1 M H_2SO_4 (thick solid line). Growth cycle numbers in each case are (in order of increase in CV size): (a, left) 1, 3, 5, 8, 10, 15, and 20 cycles; (b, center) 6, 8, 10, and 15 cycles; and (c, right) 2, 4, 6, 8, 10, 13, 16, and 20 cycles.

S0013-4651(99)11-096-6 CCC: $7.00

tain a greater amount of anodic degradation products, have a more open PANI film/Au interfacial structure, and undergo more structural changes during their growth than do type I films.[17] Therefore, a detailed impedance study of type II PANI films grown on the three different substrates was not carried out here, and CV was used as the main diagnostic technique to compare these films.

One of the differences between the CVs collected for PANI films on the three different substrates in Fig. 10 is the shape of the A_1 peak and the relative A_1 and A_2 peak heights. The ratio of these two peaks (i_{A_2}/i_{A_1}) is a measure of the extent of the degradative hydrolysis of PANI relative to the film growth, or the extent of incorporation of hydrolysis products into the PANI film.[34] Cui *et al*. measured this ratio as a function of sweep rate, electrode rotation speed, and the number of growth cycles.[34] Similarly, this ratio can be used to compare the PANI film quality as a function of substrate. On Pt (Fig. 10b), peak A_1 is relatively narrow and sharp and i_{A_2}/i_{A_1} is smaller than observed for type II PANI on both Au (Fig. 10a) and GC (Fig. 10c). Sharper, narrower peaks may indicate that the film is more homogeneous, containing chains of close to constant length, as suggested by Pickup *et al*.[31]

Another difference between the three sets of CVs in Fig. 10 is the changing potential of the first anodic peak (A_1) as a function of film growth. On Au, peak A_1 reproducibly shifts cathodically during the initial cycles, then anodically, cathodically, and then finally anodically again (Fig. 10a). No such change in peak potential was observed for PANI on Pt substrates (Fig. 10b). On GC (Fig. 10c), the CV shape is very different from both Au and Pt. With continuous potential cycling, the A_1 and C_1 redox peaks shift anodically, while the A_3 and C_3 peaks decrease in intensity (Fig. 10c). After some time of growth at GC (*e.g.*, 8th cycle), peak A_1 increases at a slower rate than A_2, while on Au and Pt, all peaks increase at a constant rate. Further growth of type II PANI film on GC would be predicted to result in the development of a single pair of redox peaks, since A_1 is shifting anodically, merging with A_2. Most of the literature shows the final CV of PANI films, instead of the series of CVs obtained during growth. Therefore, the observations and comparisons of Fig. 10 have not been reported before, especially for type II films.

The fact that type II PANI films are grown by cycling to very high potentials is clearly the cause of these three distinctly different CV responses. At potentials greater than *ca*. 1.1 V, PANI is in its fully oxidized, insulating state. Thus it is reasonable to assume that the current, during PANI growth, is driven to the underlying electrode/solution interface at the base of the PANI film pores. Therefore, type II PANI film growth will occur predominantly at the underlying electrode surface. This is supported by the fact that the underlying substrate electrochemistry can still be seen in the presence of overlying type II PANI films.

This is seen best for Au by the appearance of the Au oxide redox peaks throughout the PANI film growth period (Fig. 10a). It would not be surprising, then, to observe that the nature of the substrate notably affects the growth CVs of type II PANI films. In contrast, the CVs for type I films display only minor substrate effects, probably because film growth occurs when PANI films are conducting (*ca*. 0.9-1 V) and thus, mainly at the outer PANI film surface. Furthermore, because the shifts in peak potentials with type II PANI film thickness have a characteristic pattern for each substrate, they may indicate that unique structural rearrangements are occurring at the substrate/PANI interface during type II PANI film growth.

As the GC surface lacks a barrier oxide layer, which begins to form at Pt and Au at *ca*. 1 and 1.3 V, respectively,[35-37] type II PANI film growth rate at the underlying GC substrate is more rapid than on Au and Pt. Similarly, the rate of formation of the hydrolysis products (*e.g.*, BQ), formed either from the reaction of water with the highest oxidation state of PANI (pernigraniline) or with the oxidized aniline monomer, is higher on GC compared to that on Au and Pt. Therefore, more degradation product would be incorporated into the film during type II PANI growth on GC *vs*. on Au and Pt, consistent with the CVs. The anodic shift of E_{p,A_1} and the merging of the A_1 and A_2 peaks, seen for type II PANI films on GC, is similar to that observed during the degradation of type I PANI films on Au,[18] also supporting this suggestion.

Type II PANI films, freshly formed on GC, differ from the degraded type I PANI films on Au [18] in that type II PANI films on GC still display electrochromism and are therefore still conductivity switching. The conductivity of type II PANI films may be different from type I films, however, due to the incorporation of degradation products. Furthermore, type II PANI films formed on all substrates studied do not show a prepeak, while it is present even for a degraded type I PANI film. This suggests that the state of the substrate/polymer region, and not simply the film conductivity or porosity, is quite different. The absence of a prepeak causes the onset potential of peak A_1 to be more positive for type II than type I films (Fig. 2), so that the switching on of the film conductivity for type II films may be delayed compared to type I films.

Other factors which may influence the characteristics of both type I and type II PANI film growth include the adhesive strength of aniline to the substrate and the presence of adsorbed electrolytes. Huong *et al*.[38] reported that aniline binds strongly to Au, via a chemical interaction, and that its adsorption free energy (-47 kJ mol^{-1}) is greater than that for aniline on Hg or pyridine on Au.[38] It is likely that the strength of aniline adsorption on Pt is similar to Au, although aniline may have to compete with hydrogen for Pt sites. Furthermore, it is reasonable to infer from Lin *et al*.'s work with RuO_2 [14] that aniline adsorption on GC should be stronger than on Au and Pt. Strong aniline adsorption retards the polymerization rate.[14] This may be the main factor contributing to the slow growth of type I PANI films on GC *vs*. at Au and Pt.

For type II PANI films, aniline adsorption likely plays a less important role, compared to the influence of the barrier oxide film on Pt and Au, in affecting the characteristics of PANI film growth. Because type II films are grown by cycling to very high anodic potentials, any adsorbed aniline present will be oxidized to its radical cation and subsequently polymerized.

Conclusions

The properties of two different types of PANI films, grown by cycling the potential in 1 M H_2SO_4 on three different substrates, Pt, Au, and glassy carbon (GC), were compared using CV and ac impedance techniques. For type I films, grown by cycling between 0 and 1 V, the impact of the substrate electrode on the PANI properties is subtle. However, the results clearly show that type I PANI films grown on Pt exhibit the most rapid redox kinetics and yield the highest pseudocapacitance (per unit charge) in small potential amplitude (ac impedance) experiments. Type I PANI films, grown on Pt and Au, are significantly lower in their porosity (*ca*. 45-50%) that when formed on GC electrodes (*ca*. 77%), under the conditions of our experiments. This is correlated with their rate of growth, being most rapid on Au and Pt, and slowest on GC. The initiation of type I PANI film growth on GC is the slowest because of the apparent strong adsorption of aniline on GC and the effect of the presence of surface functionalities on the GC surface. Also, the surface coverage of type I PANI on Au and Pt is independent of film thickness, while it increases with coverage in the case of GC substrates.

Type I PANI film growth occurs when PANI is in its conducting state and hence, growth is expected to occur at the PANI/electrolyte interface, where the field is distributed. Growth of type II films, formed in 1 M H_2SO_4 by cycling the potential between 0 and 1.7 V, on the other hand, is suggested here to occur primarily at the substrate/solution interface. PANI is conducting only over a narrow range of potential (0.95 to 1.1 V), while it is insulating at above 1.1 V, and therefore film deposition would be expected to occur at the underlying metal/solution interface. It is not surprising, then, to observe a much more pronounced effect of the substrates on the characteristics of type II PANI films.

The presence of a barrier oxide layer on Pt and Au, but not on GC, is one of the main factors influencing the growth rate and characteristics of type II PANI films. As a result, type II PANI film growth is more rapid on GC than on Au and Pt, opposite to the case for type I

S0013-4651(99)11-096-6 CCC: $7.00

PANI. Also, the growth CVs show an anodic shift only in the main redox peak potential ($E_{p,A1}$) with growth of type II PANI films on GC, while on Au, both the anodic and cathodic peak potentials shift with film thickness. On Pt, $E_{p,A1}$ remains static as type II PANI films thicken. Also, the CV response of type II PANI films indicates that films on GC have the highest content of benzoquinone degradation products and the highest water content, being the most porous.

Acknowledgments

The authors are grateful to the Natural Sciences and Engineering Research Council of Canada (NSERC) for their overall support of this work. H.N.D. also acknowledges scholarship support from NSERC, IODE, Alberta Heritage Foundation, A.S.M. International Calgary Chapter, and the University of Calgary. The authors also wish to thank Dr. P. Vaný sek for access to ac impedance equipment and for useful discussions.

The University of Calgary assisted in meeting the publication costs of this article.

References

1. W. S. Huang, B. D. Humphrey, and A. G. MacDiarmid, *J. Chem. Soc., Faraday Trans. 1*, **82**, 2385 (1986).
2. B. Wang, J. Tang, and F. Wang, *Synth. Met.*, **18**, 323 (1987).
3. G. Horányi and G. Inzelt, *J. Electroanal. Chem.*, **264**, 259 (1989).
4. G. Sandí and P. Vaný sek, *Synth. Met.*, **64**, 1 (1994).
5. B. Pfeiffer, A. Thyssen, and J. W. Schultze, *J. Electroanal. Chem.*, **260**, 393 (1989).
6. T. Boschi, G. Montesperelli, P. Nunziante, G. Pistoia, and P. Fiordiponti, *Solid State Ionics*, **31**, 281 (1989).
7. A. D. Jannakoudakis, P. D. Jannakoudakis, N. Pagalos, and E. Theodoridou, *Electrochim. Acta*, **38**, 1559 (1993).
8. A. Calderone, R. Lazzaroni, and J. L. Brédas, *Synth. Met.*, **55-57**, 4620 (1993).
9. S. K. Dhawan, M. K. Ram, B. D. Malhotra, and S. Chandra, *Synth. Met.*, **75**, 119 (1995).
10. G. Mengoli, M. T. Munari, and C. Folonari, *J. Electroanal. Chem.*, **124**, 237 (1981).
11. B. Wessling, *Adv. Mater.*, **6**, 226 (1994).
12. C. M. A. Brett, A. M. C. F. O. Brett, J. L. C. Pereira, and C. Rebelo, *J. Appl. Electrochem.*, **23**, 332 (1993).
13. R. M. G. Rajapakse, A. D. L. Chandani, L. P. P. Lankeshwara, and N. L. W. L. Kumarasiri, *Synth. Met.*, **83**, 73 (1996).
14. S. M. Lin and T. C. Wen, *Electrochim. Acta*, **39**, 393 (1994).
15. H. N. Dinh and V. I. Birss, *J. Electroanal. Chem.*, **443**, 63 (1998).
16. F. Mansfeld, S. Lin, Y. C. Chen, and H. Shih, *J. Electrochem. Soc.*, **135**, 906 (1988).
17. H. N. Dinh, P. Vaný sek, and V. I. Birss, *J. Electrochem. Soc.*, **146**, 3324 (1999).
18. H. N. Dinh, J. Ding, S. J. Xia, and V. I. Birss, *J. Electroanal. Chem.*, **459**, 45 (1998).
19. T. Kobayashi, H. Yoneyama, and H. Tamura, *J. Electroanal. Chem.*, **177**, 293 (1984).
20. A. Oberlin, in *Chemistry and Physics of Carbon*, B. A. Thrower, Editor, pp. 1-43, Marcel Dekker, Inc., New York (1989).
21. H. P. Dai and K. K. Shiu, *J. Electroanal. Chem.*, **419**, 2207 (1996).
22. S. H. Pine, *Organic Chemistry*, 5th ed., McGraw-Hill Book Company, New York (1997).
23. H. N. Dinh, P. Vaný sek, and V. I. Birss, *Electrochim. Acta*, In preparation.
24. W. Scheider, *J. Phys. Chem.*, **79**, 127 (1975).
25. O. Genz, M. M. Lohrengel, and J. W. Schultze, *Electrochim. Acta*, **39**, 179 (1994).
26. M. Grzeszczuk and P. Poks, *J. Electroanal. Chem.*, **387**, 79 (1995).
27. S. H. Glarum and J. H. Marshall, *J. Electrochem. Soc.*, **134**, 142 (1987).
28. G. Inzelt, G. Lang, V. Kertesz, and J. Bacskai, *Electrochim. Acta*, **38**, 2503 (1993).
29. P. Fiordiponti and G. Pistoia, *Electrochim. Acta*, **34**, 215 (1989).
30. J. R. Macdonald, *Impedance Spectroscopy: Emphasizing Solid Materials and Systems*, John Wiley & Sons, Inc., New York (1987).
31. X. Ren and P. G. Pickup, *J. Electroanal. Chem.*, **372**, 289 (1994).
32. I. Rubinstein and E. Sabatani, *J. Electrochem. Soc.*, **134**, 3078 (1987).
33. M. Grzeszczuk and G. Zabinska-Olszak, *J. Electroanal. Chem.*, **359**, 161 (1993).
34. C. Q. Cui, L. H. Ong, T. C. Tan, and J. Y. Lee, *Electrochim. Acta*, **38**, 1395 (1993).
35. H. Angerstein-Kozlowska, B. E. Conway, and W. B. A. Sharp, *J. Electroanal. Chem.*, **43**, 9 (1973).
36. H. Angerstein-Kozlowska and B. E. Conway, *J. Electroanal. Chem.*, **228**, 429 (1987).
37. M. E. Vela, R. C. Salvarezza, and A. J. Arvia, *Electrochim. Acta*, **35**, 117 (1990).
38. C. N. V. Huong, *J. Electroanal. Chem.*, **264**, 247 (1989).